Mathematical Theory of Decaying Turbulence

Alexander Migdal

Institute for Advanced Study, Princeton, USA

Rurtgers Mathematical Physics Seminar, March 27, 2025

Established Theories and Unsolved Problems

- About 50 years ago, I visited Rutgers and Princeton for the first time. This marked the beginning of enduring scientific collaborations intertwined with lasting personal friendships.
- Theoretical physics was black and white back then. A clear consensus existed on fundamental theories: **Gibbs Statistics, Relativity, Quantum Mechanics, Classical Gravity, and the Standard Model**.
- Everyone acknowledged two major unsolved problems: **Quantum Gravity and Turbulence**. The first has resisted all efforts of the best minds for the last century.
- The second problem, however, **has now been solved**, and today I will present this solution, contradicting some widely held beliefs within the turbulence community.
- The **String Theory/QFT** community may find it easier to accept, as it is a manifestation of **duality**, much like **AdS/CFT**.

The Old Road to Turbulence

Discovery Year	Portrait	Key Contribution
1500s		**Leonardo da Vinci**: Documented early observations of turbulent flow.
1820s	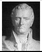 	**Claude-Louis Navier** and **George Gabriel Stokes**: Formulated the foundational NS equations.
1883		**Osborne Reynolds**: Characterized the transition to turbulence.
1941		**Andrey Kolmogorov**: Proposed scaling laws of turbulence (**K41**).
1944		**Werner Heisenberg**: Theoretical contributions to stability and dissipation models.
1946		**Lars Onsager**: Introduced insights into fractal velocity fields and vortex structures.
1948-1952		**Eberhard Hopf**: The functional equation for statistics of turbulence.
1956		**Lev Landau**: Advanced the understanding of hydrodynamic stability.
1985	 	**Giorgio Parisi** and **Uriel Frisch**: Proposed multifractal models for turbulence.
2000-2022		**K.R. Sreenivasan**: DNS studies uncovering **scaling law violations**.

Scaling Law Violations: The Dead End of the Old Road

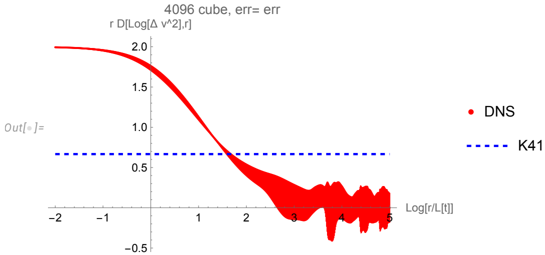

Key Findings

- **Kolmogorov's K41 model theory** predicted universal scaling laws for velocity difference moments, including an index of $2/3$ for the second moment.
- This figure shows the effective index $=$ logarithmic derivative of the second moment $\left\langle \Delta \vec{v}^2(r,t) \right\rangle$ plotted against $\log(r/\sqrt{t})$.
- DNS simulations (4096^3 **lattice, 2024**) using a novel method to extract effective indices from observed energy spectra [12] **contradicted any scaling law** (a horizontal line on this plot).

From Phenomenology to First Principles

- A central question remains: **How does randomness emerge from deterministic Navier-Stokes dynamics?**
- Answering this requires a **direct, exact solution** of the Navier-Stokes equations, rather than relying on phenomenological models.
- Efforts toward this goal began in the 1990s with **loop equations** [11], inspired by breakthroughs in quantum chromodynamics (QCD) [8, 2].
- These advances culminated in a **first-principles mathematical theory** for decaying turbulence, reducing the inherently three-dimensional PDE to a one-dimensional dynamical system governed by an algebraic fixed-point equation.
- This dimensional reduction introduced the **Euler ensemble**, a solvable string theory that quantitatively describes decaying turbulence, marking a decisive detour into a new paradigm beyond K41.
- The theory predicts **generalized scaling laws** with an infinite spectrum of decay indices, which are **computed analytically** and agree with experimental data.
- The answer to the randomness question mirrors **Maxwell-Gibbs statistics**: the Navier-Stokes trajectory covers the degenerate fixed point, corresponding to the **Euler ensemble**.
- The key novelty lies in the discrete nature of this fixed point, which contrasts sharply with the continuous energy surface of classical statistical mechanics.

Loop Average and Dimension Reduction

- The loop average is defined as the **characteristic function** for the distribution of velocity circulation:

$$\Psi[\gamma, C] = \left\langle \exp\left(\frac{\imath\gamma}{\nu}\Gamma_C\right)\right\rangle, \quad \Gamma_C = \oint d\vec{C}(\theta) \cdot \vec{v}(\vec{C}(\theta)).$$

- This is a particular case of the **Hopf functional** representation:

$$\Psi[\gamma, C] = \left\langle \exp\left(\int_{\vec{r} \in \mathbb{R}^3} \vec{J}_C(\vec{r}) \cdot \vec{v}(\vec{r})\, d^3 r\right)\right\rangle.$$

- An imaginary source $\vec{J}(\vec{r})$ is concentrated on a fixed loop in space $\mathbb{R}_3$

$$\vec{J}_C(\vec{r}) = \frac{\imath\gamma}{\nu} \oint d\vec{C}(\theta) \delta^3\left(\vec{r} - \vec{C}(\theta)\right)$$

Loop Equation as Quantum Mechanics in Loop Space

- The loop functional satisfies a key relation derived from the incompressible Navier-Stokes equation:

$$\imath\nu\partial_t\Psi[\gamma, C] = \left\langle \gamma \oint d\vec{C}(\theta)\cdot\left(-\nu\vec{\nabla}\times\vec{\omega}+\vec{v}\times\vec{\omega}\right)e^{\frac{\imath\gamma}{\nu}\Gamma_C}\right\rangle.$$

- This relation leads to the closed functional equation for the loop average [11]:

$$\imath\nu\partial_t\Psi[\gamma, C] = \oint d\vec{C}(\theta)\cdot\vec{L}\left[\frac{\delta}{\delta\vec{C}(\cdot)}\right]\Psi[\gamma, C].$$

- A crucial property: **translation invariance** of $\vec{L}\left[\frac{\delta}{\delta\vec{C}(\cdot)}\right]$ in loop space enables an exact solution.

Key Insight: Plane Wave Solutions in Loop Space

- The loop equation maps fluid dynamics to a **Schrödinger equation in loop space** with a Hamiltonian:

$$\hat{H}_C = \oint d\vec{C}(\theta) \cdot \vec{L}\left[\frac{\delta}{\delta \vec{C}(\cdot)}\right].$$

- A **plane wave solution** emerges naturally:

$$\Psi[\gamma, C] = \left\langle \exp\left(\frac{\imath\gamma}{\nu} \oint d\vec{C}(\theta) \cdot \vec{P}(t,\theta)\right)\right\rangle_{P(t)}.$$

- The averaging $\langle \dots \rangle_{P(t)}$ goes over solutions of the following momentum loop equation (MLE), with $\Delta\vec{P} = \vec{P}(\theta_+) - \vec{P}(\theta_-)$ being a discontinuity:

$$\nu \partial_t \vec{P} = -\gamma^2 (\Delta\vec{P})^2 \vec{P} + \Delta\vec{P}\left(\gamma^2 \vec{P} \cdot \Delta\vec{P} + \imath\gamma \left(\frac{(\vec{P} \cdot \Delta\vec{P})^2}{\Delta\vec{P}^2} - \vec{P}^2\right)\right).$$

The Euler Ensemble Solves MLE

- The decaying solution of MLE [13] is given by:

$$\vec{P}(t,\theta) = \sqrt{\frac{\nu}{2(t+t_0)}}\frac{\vec{F}(\theta)}{\gamma},$$

  where $\vec{F}(\theta)$ is a **universal fractal curve**, constructed as the limit $N \to \infty$ of a regular star polygon $\{q/p\}$ with vertices: $\vec{F}\left(\frac{2\pi k}{N}\right) = \hat{\Omega}\cdot\frac{\{\cos(\alpha_k),\sin(\alpha_k),\imath\cos(\frac{\beta}{2})\}}{2\sin(\frac{\beta}{2})}$, where: $\beta = \frac{2\pi p}{q}$, $\alpha_k = \beta\sum_{l=0}^{k}\sigma_l$, $k = 1,\dots N, \quad N \to \infty$

- The parameters $\hat{\Omega} \in SO(3), \frac{p}{q} \in \mathbb{Q}, \sigma_k = \pm 1$ are **random**, making $\vec{P}(t,\theta)$ a **fixed stochastic trajectory** of MLE.
- This solution is equivalent to a **random walk on the set of regular star polygons**.
- **Validation:** This solution has been verified using *Mathematica®* notebooks [9] and rigorously tested in collaboration with mathematicians [6].
- **Significance:** This framework quantitatively **links turbulence to number theory**, providing a fresh perspective on fluid dynamics.

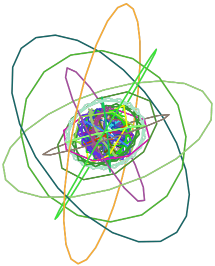

Spontaneous Quantization of Classical Turbulence

Chaotic Vortex Motion

Random Walk on Star Polygons

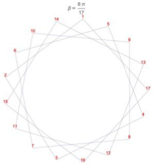

- A **thirty-year effort** culminated in 2023 in an **exact, universal solution** to the Navier-Stokes equations in the turbulent regime [13].
- This solution reveals a **duality** between decaying turbulence and a solvable string theory with a **discrete target space**: random walk on regular star polygons.
- Turbulent randomness arises from **spontaneous quantization**, where discrete parameters emerge from a **manifold of solutions of MLE and periodicity requirement**.
- **Universal number-theoretic functions** now quantitatively explain DNS data violations of classical scaling laws, providing a **predictive framework** for turbulence [12].

Regular Star Polygons of the Euler Ensemble

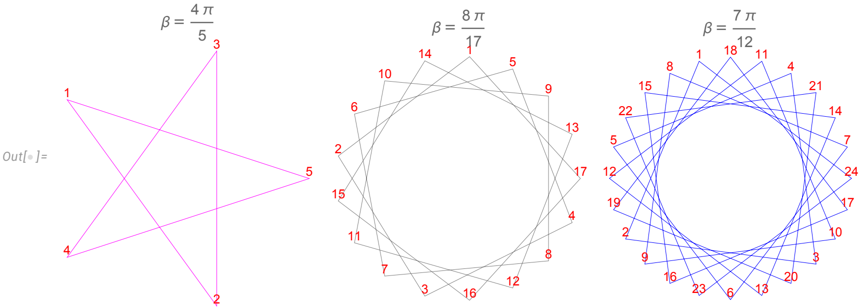

Description

Regular star polygons with various p, q.

These were first classified by **Thomas Bradwardine** (c. 1300 – 1349), Archbishop of Canterbury.

The σ_k **variable** governs the direction of the random step along the link $k \leftrightarrow k+1$.

The **random walk** can traverse the polygon multiple times, provided it returns to its starting point.

Random Walk on Star Polygon, $p = 7, q = 18, N = 100$

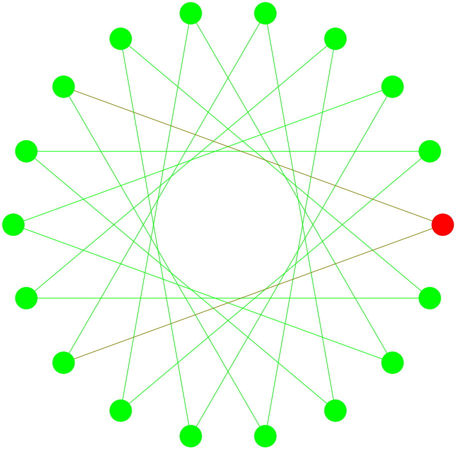

Visualization

Visualization of a **random walk** on a star polygon with parameters $p = 7$, $q = 18$, and $N = 100$.

The Quantum Ergodic Hypothesis

- The characteristic function Ψ of a probability distribution P equals the complex wave function of quantum mechanics in loop space. This relation is exact, and it differs from conventional $P = |\Psi|^2$.
- Each **distinct state** in a quantum system contributes to the partition function with unit weight, a principle adopted in our **quantum description** of the nonlinear NS system.
- This **uniform measure** is an **additional conjecture**, comparable to the ergodic hypothesis in Newtonian mechanics. While well-established in physics, such hypotheses are mathematically proven only for specific cases.
- The heuristic argument for our quantum ergodic hypothesis is the equivalence of the Euler ensemble to the string theory with discrete target space.

Turbulence/String Duality: Insights

- **Duality phenomena** in physics connect strong coupling in one theory to weak coupling in another, as seen in the **AdS/CFT correspondence**.
- Duality links **statistical averages** between two systems without requiring a direct mapping of their dynamical variables.
- In turbulence, the **target space** of the dual string theory is discrete, represented by **regular star polygons** with unit sides and rational angles, $\beta = 2\pi\frac{p}{q}$.
- Fermionic or Ising degrees of freedom $(\nu_k = 0, 1;\ \sigma_k = \pm 1)$ describe the random walk along polygon edges.
- The radii of these polygons, $R = \frac{1}{2\sin\pi\frac{p}{q}}$, follow number-theoretic distributions involving Euler totients and the Riemann ζ function [12].
- This isn't your grandfather's string theory—it exists in 3D.

Dual Amplitude and Loop Functional

- The loop functional in the Euler ensemble corresponds to the **dual amplitude** of string theory, defined on a discrete target space $\vec{F}(\theta)$ with distributed external momentum $\vec{Q}(\theta,t) = \frac{\vec{C}'(\theta)}{\sqrt{2\nu(t+t_0)}}$:

$$\Psi[C,t] = \left\langle \exp \imath \oint d\theta \vec{F}(\theta) \cdot \vec{Q}(\theta,t) \right\rangle_{F,\sigma}$$

- Averaging over **string target space** $\vec{F}_k$ corresponds to summing over star polygons with unit sides and rational angles $\beta = 2\pi \frac{p}{q}$.
- Averaging over **fermionic/Ising degrees of freedom** produces a random walk (Brownian motion in the continuum limit) across polygon vertices.
- The viscosity enters this string theory as a coupling constant in the denominator of the effective Action. The turbulent limit of $\nu \to 0$ becomes the weak coupling limit, solvable in the WKB approximation.

Discrete Symmetry and Target Space Integration

- **Key contrast:** Turbulence features chaotic velocity fields mapping $\mathbb{R}_3 \mapsto \mathbb{R}_3$, whereas the dual string theory has discrete variables $\vec{F}, \sigma$ mapping the unit circle to discrete sets $\mathbb{S}_1 \mapsto \mathbb{Q}, \mathbb{S}_1 \mapsto \mathbb{Z}_2$.
- Integration over the target space (star polygons) reduces to a **discrete sum** over Euler ensemble states:
  - Rational numbers $\frac{p}{q} \in \mathbb{Q}$,
  - Ising variables $\sigma_k = \pm 1$,
  - Winding number $w = \frac{p}{q} \sum \sigma_k$.
- Visualizing the polygons for fixed N, ordered by angle β, as a torus in 3D space reveals the **world sheet** of a discrete string. Each polygon forms a cross-section of the torus:
  - Smaller cross-sections correspond to small p, q.
  - Larger cross-sections arise as $q \to \infty$, with p or $q - p$ held fixed.
- Red/green edge coloring indicates random walk directions σ_k.

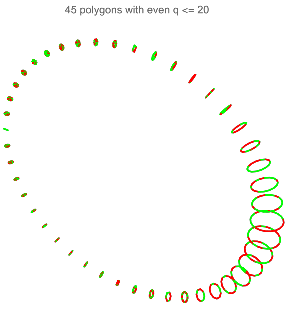

Revealing a Hidden Identity

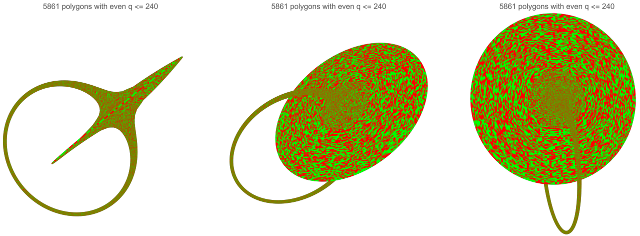

- We are not merely computing turbulence statistics but **unveiling its hidden second identity as a discrete string theory**.
- Existing experimental and DNS results show **encouraging agreement** with the predictions of the Euler ensemble.
- This theory challenges traditional views developed over the past eighty years, inviting rigorous scrutiny.
- Ultimately, **large-scale numerical and physical experiments** will determine whether this theory fully describes turbulence or remains a beautiful mathematical model.

The Warning Signs for K41: Sreeni's Observations

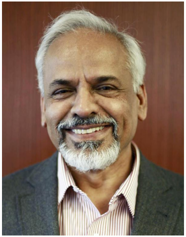

- In his 2023 ICTS talk, **K.R. Sreenivasan** reviewed DNS data on decaying turbulence, discussing its alignment with **classical scaling laws (Kolmogorov-Saffman)**.
- He noted **persistent discrepancies**, regretting that the results were "not more closely aligned with theoretical arguments".
- The key DNS dataset, briefly mentioned in passing in an earlier paper, remained unpublished but contained clues to unresolved questions in turbulence theory.
- Sreeni took the initiative to share with me his raw data from a private archive, sparking a productive collaboration.

A Refined Analysis: Effective Index Method

- Using the **effective index method**, I magnified subtle discrepancies in DNS data, demonstrating strong violations of the **Kolmogorov scaling law (K41)** in decaying turbulence.
- This method introduced a **Fourier integral representation** [12] for the effective scaling index, **reducing statistical noise** and significantly improving data clarity.
- The analysis revealed a **remarkable agreement** between DNS data and the Euler ensemble's predictions, providing evidence for the absence of a **classical inertial range**.
- The historical reliance on K41 scaling in decaying turbulence likely stemmed from attempts to **force unfitting pieces of the puzzle** into this framework, attributing deviations to **"deep dissipation effects."**
- What once seemed like scattered puzzle pieces now aligns seamlessly within the **Euler ensemble framework**, offering a complete and coherent picture of turbulence.

Verification by DNS (Sreenivasan et. al., 2025)

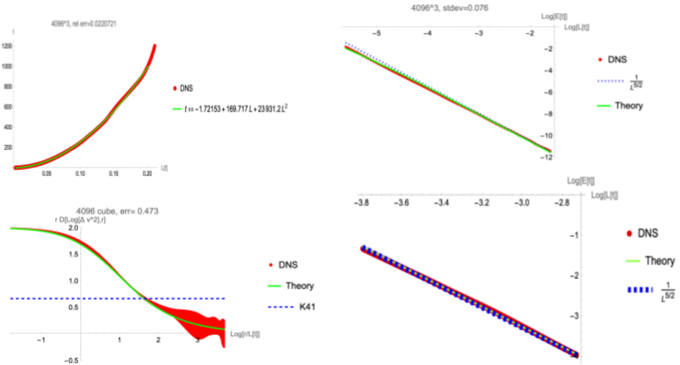

DNS Data Explained

- The lower-left panel shows the log derivative of the second velocity moment:
$$r\partial_r \log \left\langle (\vec{v}(\vec{r},t) - \vec{v}(0,t))^2 \right\rangle ,$$
comparing predictions from the **Euler ensemble** (green curve) and **DNS data** (red curve with error bars).
- **Key Insight:** Predictions from the Euler ensemble closely match DNS results, while **Kolmogorov scaling** (dashed blue line) fails, confirming the absence of a classical inertial range.
- Multifractal models, though offering vertical shifts of the horizontal K41 line, still contradict the observed nonlinear curve.
- Additional panels illustrate:
  - **Upper-left:** The relationship between time and effective length scale.
  - **Upper- and lower-right:** The relationship between decaying kinetic energy and effective length.
- **Summary:** The **Euler ensemble**, with no adjustable parameters, reproduces DNS data within experimental error margins.

Experimental Data: Inverse Energy Scaling

Decaying Energy Multi Scaling laws

$$\Delta_p$$

Leading $\rightarrow$

$$\left|\begin{array}{c} -\frac{5}{4} \\ -\frac{11}{4} \\ \boxed{-\frac{7}{2} \pm \frac{\imath}{2} t_n \text{ if } n \in \mathbb{Z}} \\ \boxed{-\frac{15}{4} - n \text{ if } n \in \mathbb{Z} \land n \geq 0} \\ \hline \boxed{\frac{n}{2} \text{ if } n \in \mathbb{Z} \land n \geq 0} \end{array}\right|$$

$$\zeta\left(\frac{1}{2} + \imath t_n\right) = 0$$

$$E(t) \propto \sum \Re A_p t^{\Delta_p}$$

Kolmogorov-Saffman model: 6/5 = 1.2

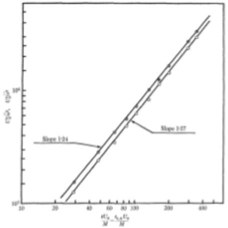

Comte-Bellot G, Corrsin S. data: 1.25

Experimental Data Explained

- Theoretical predictions for **decaying turbulent kinetic energy indices** from the **Euler ensemble** are shown on the left. The leading index is $-5/4$, accompanied by an **infinite series** of additional negative indices.
- Experimental data [4, 5] for **decaying turbulence behind an oscillating grid** is displayed on the right.
- Log-log plots illustrate $1/v_\perp^2$ and $1/v_\parallel^2$, corresponding to the perpendicular and parallel velocity components.
- Total inverse kinetic energy, $K = 2/(v_\perp^2 + v_\parallel^2)$, exhibits a slope of 1.255 ± 0.02, in excellent agreement with the Euler ensemble prediction of $\frac{5}{4}$.
- Recent experiments using a **large tank setup** [7] independently confirm this **decay index**, providing strong support for the theory.
- In both experiments, the authors **observed** a decay index of 1.25, but **claimed agreement** with the Kolmogorov-Saffman (K-S) scaling law (1.2), which lies outside their stated error margin.
- For decades, these contradictions between data and K41-based assumptions were **overlooked**, highlighting how entrenched theoretical frameworks can hinder critical evaluation.
- **Summary:** The predicted energy decay index $-5/4$ aligns with experimental data, while the K-S index $-6/5$ is inconsistent with the observed results.

Explicit Formula for Velocity Correlation

The statistical limit of the Euler ensemble as $N \to \infty, \nu \to 0, \tilde{\nu} = \nu N^2 =$ *const* , enables computations of the energy spectrum and correlation functions in quadrature.

Here is the resulting **formula for the second moment of velocity difference**:

$$\left\langle \Delta \vec{v}^2 \right\rangle (r,t) = \frac{\tilde{\nu}^2}{\nu t} \int_{\epsilon - \imath\infty}^{\epsilon + \imath\infty} \frac{dp}{2\pi\imath} V(p) \left(\frac{|\vec{r}|}{\sqrt{\tilde{\nu} t}} \right)^p ;$$

$$V(p) = -\frac{f(-1-p)\zeta\left(\frac{13}{2} - p\right)\csc\left(\frac{\pi p}{2}\right)}{16\pi^2 (p+1)(2p-15)(2p-5)\zeta\left(\frac{15}{2} - p\right)}. \tag{1}$$

Here $f(z)$ is an entire function computed via Mellin integrals of elementary functions. $V(p)$ is meromorphic. ν is physical viscosity, while turbulent viscosity $\tilde{\nu}$ is a free parameter of the solution.

Spectrum of indices of velocity correlation

The spectrum of indices for velocity correlation is given by the poles of $V(p)$

indexes of velocity correlation

Index	Condition
-1	
0	
$2n$	$n \in \mathbb{Z}, n \geq 1$
$5/2$	
$11/2$	
$\frac{15+4n}{2}$	$n \in \mathbb{Z}, n \geq 0$
$7 \pm \imath t_n$	$n \in \mathbb{Z}$

(2)

where $\frac{1}{2} \pm \imath t_n$ are the **zeros of the Riemann ζ function**.

Quantum oscillations predicted

- As mentioned about the energy spectrum, there is no K41 scaling index $p = \frac{2}{3}$. This omission is not a contradiction, as K41 does not apply to decaying turbulence.
- Instead of pure scaling laws with a single decay index each, we found an **infinite spectrum of scaling indexes**, some of which come as complex conjugate pairs, which leads to **quantum oscillations** of the index at large $r/\sqrt{t}$.
- The imaginary parts of these complex scaling dimensions coincide with those of the **famous Riemann zeta zeros**, establishing an intriguing relation between Turbulence and Number Theory.
- These oscillations are inaccessible with the modern lattice sizes in the DNS, but rather would require lattices like $24K$, available in near future.

Quantum Oscillations Predicted

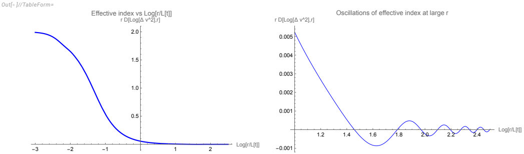

- Oscillations of the effective index $\xi_2(r)$ at large $\log_{10} r$. This is a theoretical curve corresponding to the zoom into a region of large separations, currently inaccessible by DNS with the required accuracy.
- This quantum-like behavior in classical turbulence is rather unexpected but fascinating.
- It stems from **precise mathematical equivalence** of the evolution of the characteristic function of the velocity circulation to the quantum mechanics in loop space, creating the interference of alternative histories.
- Quantitative description of the oscillating effective index follows from the statistical limit of the Euler ensemble, governed by the number theory.

Spectrum of decay indices of energy spectrum

$$
\begin{array}{|c|}
\text{energy spectrum indexes} \\
\hline
-\frac{7}{2} \\
-\frac{13}{2} \\
\boxed{-8 \pm \imath t_n \text{ if } n \in \mathbb{Z}} \\
\boxed{-\frac{17}{2} - 2n \text{ if } n \in \mathbb{Z} \land n \geq 0} \\
\hline
\boxed{n \text{ if } n \in \mathbb{Z} \land n \geq 0}
\end{array}
\tag{3}
$$

Here $\pm t_n$ are imaginary parts of zeros of the ζ function on the critical line $z = \frac{1}{2} + \imath t$.

- The energy spectrum decays as $t^{-\frac{9}{4}} k^{-\frac{7}{2}}$.
- There is no theoretical reason (even at the level of heuristic) for K41 in decaying turbulence, as the dissipation $\mathcal{E}(t)$ is not a constant, so it cannot be used as a single scaling parameter.
- DNS and experiments also point at large deviations from the $k^{-5/3}$ scaling law in decaying turbulence [15].

AI-Driven Open Source Project for Turbulence Research

- Due to the **computational intensity** required to calculate the statistical limits of the Euler ensemble, manual methods are **inefficient**.
- To overcome this, we are initiating an **open source project on GitHub**[14] with the following objectives:
  - **Further expand and validate** the Euler ensemble framework through community involvement.
  - Create a **collaborative platform** for sharing ideas, providing feedback, and making constructive contributions.
- Key features of this project include:
  - An **interactive, comprehensive database** containing *Mathematica*® notebooks, research articles, experimental datasets, and DNS simulation results.
  - An **AI-enhanced interface** designed to facilitate exploration of theoretical models, perform computations, and analyze experimental outcomes.
  - **High-performance computing capabilities** utilizing *Mathematica*® for complex calculations.

The Future Directions and Remaining Problems

- The **equivalence between decaying turbulence and solvable string theory** offers a **novel perspective** in fluid mechanics.
- This framework provides tools for analyzing:
  - **Turbulence in $d > 3$ dimensions** (solved)[13].
  - **Magnetohydrodynamic (MHD) turbulence** (solved)[10].
  - **Turbulent mixing (passive scalar)** (solved, in preparation)[1].
  - **Turbulence forced by random rotations** (solved, in preparation)[3].
  - **Compressible (aerodynamic) turbulence**.
- **Collaboration** with mathematicians, experimentalists, and DNS researchers is crucial for **extending and validating** this theory.
- **Open Questions:**
  - **What role does external forcing play** in modifying the turbulence-string duality?
  - Are there **other PDEs** with similar dimensional reductions?
  - How can the **Euler ensemble** be generalized for random walks on loop groups?

Closing Thoughts: The Ascent to Understanding

- Scaling the summit of turbulence theory is like climbing up the Matterhorn.
- Each milestone—loop equations, dimension reduction, and Euler ensemble—brings us closer to a breathtaking view at the summit.
- The wing-suit figure is me: flying or falling? The landing will tell...

References I

[1] A. Migdal. *Dual Theory of Turbulent Mixing*. "In preparation". 2025.

[2] A. Migdal. " Loop equations and $\frac{1}{N}$ expansion". In: *Physics Reports* 201 (1983).

[3] A. Migdal. *Quantum Solution of Classical Turbulence Forced by Random Rotation*. "In preparation". 2025.

[4] Geneviéve Comte-Bellot and Stanley Corrsin. "The use of a contraction to improve the isotropy of grid-generated turbulence". In: *Journal of Fluid Mechanics* 25.4 (1966), pp. 657–682. DOI: 10.1017/S0022112066000338.

[5] Geneviève Comte-Bellot and Stanley Corrsin. "Simple Eulerian time correlation of full-and narrow-band velocity signals in grid-generated, 'isotropic' turbulence". In: *Journal of Fluid Mechanics* 48.2 (1971), pp. 273–337. DOI: 10.1017/S0022112071001599.

References II

[6] C. DeLellis E. Brue and A. Migdal. *On the mathematical foundation of duality of fluid mechanics*. "In preparation". 2025.

[7] Jean-Baptiste Gorce and Eric Falcon. "Freely Decaying Saffman Turbulence Experimentally Generated by Magnetic Stirrers". In: *Phys. Rev. Lett.* 132 (26 June 2024), p. 264001. DOI: 10.1103/PhysRevLett.132.264001. URL: https://link.aps.org/doi/10.1103/PhysRevLett.132.264001.

[8] Yu.M. Makeenko and A.A. Migdal. "Exact equation for the loop average in multicolor QCD". In: *Physics Letters B* 88.1 (1979), pp. 135–137. ISSN: 0370-2693. DOI: https://doi.org/10.1016/0370-2693(79)90131-X. URL: https://www.sciencedirect.com/science/article/pii/037026937990131X.

[9] Alexander Migdal. *Decaying Turbulence Computations*. https://www.wo sasha.migdal/Published/DecayingTurbulenceComputations.nb. Sept. 2023.

References III

[10] Alexander Migdal. *Dual Theory of MHD Turbulence*. 2025. arXiv: 2503.12682 [physics.flu-dyn]. URL: https://arxiv.org/abs/2503.12682.

[11] Alexander Migdal. "Loop Equation and Area Law in Turbulence". In: *Quantum Field Theory and String Theory*. Ed. by Laurent Baulieu et al. Springer US, 1995, pp. 193–231. DOI: 10.1007/978-1-4615-1819-8. URL: https://arxiv.org/abs/hep-th/9310088.

[12] Alexander Migdal. "Quantum solution of classical turbulence: Decaying energy spectrum". In: *Physics of Fluids* 36.9 (2024), p. 095161. DOI: 10.1063/5.0228660.

[13] Alexander Migdal. "To the Theory of Decaying Turbulence". In: *Fractal and Fractional* 7.10 (Oct. 2023), p. 754. ISSN: 2504-3110. DOI: 10.3390/fractalfract7100754. arXiv: 2304.13719 [physics.flu-dyn]. URL: http://dx.doi.org/10.3390/fractalfract7100754.

References IV

[14] Alexander Migdal. *TurbulenceDuality*. https://github.com/sashamigdal/TurbulenceDuality/. Open source project for study of Turbulencve Duality. Dec. 2025.

[15] John Panickacheril John, Diego A Donzis, and Katepalli R Sreenivasan. “Laws of turbulence decay from direct numerical simulations”. en. In: *Philos. Trans. A Math. Phys. Eng. Sci.* 380.2218 (Mar. 2022), p. 20210089.

Energy Decay in the Euler Ensemble

- Solutions originating deep within the unit circle ($\Psi \neq 1$) can become turbulent and eventually decay toward $\Psi \to 1$, reflecting energy dissipation by micro-scale vortex structures.
- The decaying solution for $\vec{P}(\theta, t)$:

$$\vec{P} = \sqrt{\frac{\nu}{2(t+t_0)}}\frac{\vec{F}}{\gamma},$$

where $\vec{F}$ satisfies the fixed-point equation:

$$\left((\Delta\vec{F})^2 - 1\right)\vec{F} = \Delta\vec{F}\left(\gamma^2\vec{F}\cdot\Delta\vec{F} + \imath\gamma\left(\frac{(\vec{F}\cdot\Delta\vec{F})^2}{\Delta\vec{F}^2} - \vec{F}^2\right)\right).$$

Fractal Curve as the Euler Ensemble

- The equation for $\vec{F}(\theta)$ was solved and analyzed in [13, 12].
- The solution describes a **fractal curve**, the limit $N \to \infty$ of a polygon $\vec{F}_0 \dots \vec{F}_N = \vec{F}_0$, with vertices:

$$\vec{F}_k = \frac{\{\cos(\alpha_k), \sin(\alpha_k), \imath \cos(\frac{\beta}{2})\}}{2 \sin(\frac{\beta}{2})},$$

where:

$$\theta_k = \frac{k}{N}, \quad \beta = \frac{2\pi p}{q}, \quad N \to \infty,$$
$$\alpha_{k+1} = \alpha_k + \sigma_k \beta, \quad \sigma_k = \pm 1, \quad \beta \sum \sigma_k = 2\pi p r.$$

- Parameters $\hat{\Omega}, p, q, r, \sigma_0 \dots \sigma_N = \sigma_0$ are **random**, making $\vec{F}(\theta)$ a **fixed manifold** instead of a fixed point.
- This manifold, called the **big Euler ensemble**, highlights the degeneracy of solutions.

Fixed Point and Degeneracy

- The fixed-point equation uses discrete versions of continuity and principal value:

$$\Delta\vec{F} \equiv \vec{F}_{k+1} - \vec{F}_k,$$
$$\vec{F} \equiv \frac{\vec{F}_{k+1} + \vec{F}_k}{2}.$$

- Both terms in the fixed-point equation vanish independently, leading to two scalar conditions:

$$(\Delta\vec{F})^2 = 1, \tag{4a}$$
$$\vec{F}^2 - \frac{\gamma^2}{4} = \left(\vec{F}\cdot\Delta\vec{F} - \frac{\imath\gamma}{2}\right)^2. \tag{4b}$$

- These equations ensure nonzero vorticity, avoiding $\vec{F} \parallel \Delta\vec{F}$.

Origin of Randomness and Integers

- Randomness in the Euler ensemble does not stem from infinitesimal stochastic forces but from the **degenerate fixed manifold** of nonlinear equations.
- This internal stochasticity resembles ergodic behavior in Newtonian dynamics, where trajectories uniformly cover the energy surface, leading to Gibbs-Maxwell distributions.
- Integer solutions ($\sigma_k = \pm 1$) emerge from:
  - Algebraic constraints in the fixed-point equations.
  - Rational quantization ($\beta = 2\pi p/q$) dictated by wave function periodicity.
- Remarkably, co-prime pairs of integers p and q define the quantized angles and radii of star polygons, reminiscent of quantum effects in magnetic fields.

The Euler Totient and the Ensemble

- The integers $1 \leq p < q$ are constrained to be co-prime with q and satisfy:

$$2 < q < N, \quad (N - q) \mod 2 = 0.$$

- The number of valid fractions $\frac{p}{q}$ for a fixed q is given by the **Euler totient function**:

$$\varphi(q) = \sum_{\substack{p=1 \\ (p,q)}}^{q-1} 1 = q \prod_{p|q} \left(1 - \frac{1}{p}\right).$$

- We named this set the **Euler ensemble** to honor Euler's contributions to both fluid dynamics and number theory.
- The inviscid Navier-Stokes equation is described by the Euler totient function rather than the Euler equation itself.